Proceedings of ENCIT 2012
14th Brazilian Congress of Thermal Sciences and Engineering
November 18-22, 2012, Rio de Janeiro, RJ, Brazil

SPRAY CONE ANGLES GENERATED BY A DUAL CENTRIFUGAL INJECTOR

Roger Apaza Vásquez, roger@lcp.inpe.br
Fernando de Souza Costa, fernando@lcp.inpe.br
Laboratório Associado de Combustão e Propulsão
Instituto Nacional de Pesquisas Espaciais
Rodovia Presidente Dutra, km 40, Cachoeira Paulista, SP, 12630-000, Brasil

Abstract. *A dual pressure swirl injector is characterized by two independent concentric chambers which can provide independent rotational levels to a single liquid or two different liquids. This paper compares theoretical and experimental results concerning the spray cone angles formed by injection of water, ethanol and biodiesel through a dual pressure swirl injector. Data are obtained for injection of the same liquid through the primary and secondary chambers and for injection of ethanol in the primary chamber and biodiesel through the secondary chamber of the injector. Experimental data are obtained using photographic techniques and are analyzed by an image processing software developed in Matlab language.*

Keywords*: dual pressure swirl injector, ethanol,biodiesel, spray cone angle*

1. INTRODUCTION

Combustion of fuels in rocket engines, gas turbines, and other industrial applications depends on effective atomization of liquid fuel or oxidizer by an injector to achieve high rates of mixing and evaporation.

A simple swirl injector consists of one or more inlets into a central vortex chamber, the inlets generally being tangential, thus providing the spin in the vortex chamber. Finally the fluid emerges from an orifice in the form of a film around the periphery of the orifice; this film then breaks into a cone of spray particles. The spray of the liquid produced at the output of this type of injector has the approximate shape of a hollow-cone. (Lefebvre, 1989).

A dual pressure swirl injector is characterized by two independent concentric vortex chambers which can provide independent rotational levels to a single liquid or two different liquids. In the case of a dual pressure swirl injector a hollow-cone is formed for each chamber and when there is a collision of the two cones it is formed a single cone.

Generally when the cone angle is increased there is also an increase in the contact of droplets of liquid injected with ambient air, which improves the atomization process, the heat and mass transfer. Moreover, the reduction in the cone angle improves the performance of the ignition and extends the limits of stability (Ortmann *et al.*, 1985). The cone angle is an important external feature of a spray. Due to the interactions of the liquid fuel with air, the curve of the spray actually has the approximate shape of a bell, thus presenting the difficulty of measuring the cone angle (see Figure 1). Typically, the measurement of this external feature is defined as the angle (2α) formed by two straight lines in a plane projected from the orifice discharge of injector, at a specified distance.

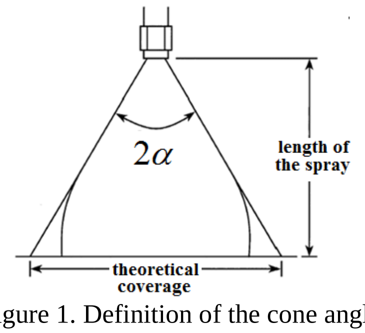

Figure 1. Definition of the cone angle.

This paper compares theoretical, semi-empirical and experimental results concerning the spray cone angles formed by injection of ethanol and biodiesel through a dual pressure swirl injector.

Data are obtained for injection of biofuels only through the primary and secondary chambers and for injection of ethanol in the primary chamber and biodiesel through the secondary chamber of the injector.

Experimental data are obtained using photographic techniques and are analyzed by a graphical user interface (GUI) written in Matlab language.

2. THEORETICAL AND SEMI-EMPIRICAL MODELS

There are several theoretical and semi-empirical models to determine the behavior of the cone angle formed by swirl injectors.

2.1 Theoretical Model

To determine the cone angle of the primary chamber it is necessary, initially, to specify the injector geometrical parameter K_{prim}:

$$K_{prim} = \frac{\pi r_s R_{prim}}{A_f} \tag{1}$$

where r_s is the outer radius of the nozzle outlet, A_f is the area of tangential holes and $R_{prim} = r_{cv\,prim} - r_{f\,prim}$, where $r_{cv\,prim}$ is the radius of the vortex chamber and $r_{f\,prim}$ is the radius of the tangencial holes.

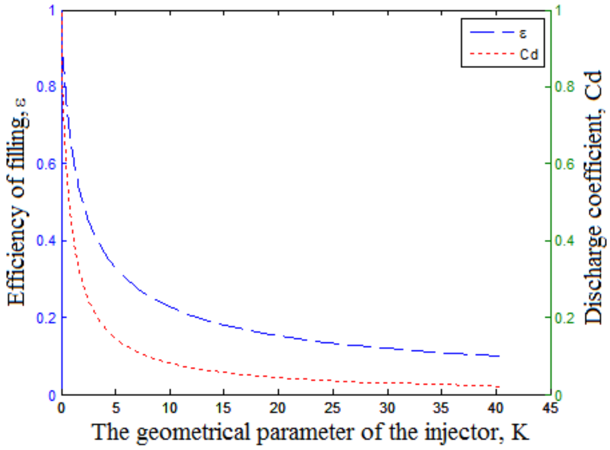

Figure 2. Behavior of geometrical parameters, the discharge coefficient and the efficiency of filling of the injector.

Using Figure 2, for a given $K_{prim} = K$ we find a value of ε, and then we compute the Z parameter:

$$Z = \frac{1}{K_{prim}} \frac{\left(1-\varepsilon_{eq\,prim}\right)\sqrt{2}}{\varepsilon_{eq\,prim}\sqrt{\varepsilon_{eq\,prim}}} \tag{2}$$

An equivalent discharge coefficient is determined using the equation (Vasquez, 2011):

$$C_{deq\,prim} = \frac{\varepsilon_{eq\,prim}\sqrt{\varepsilon_{eq\,prim}}}{\sqrt{2-\varepsilon_{eq\,prim}}} \tag{3}$$

Then the final discharge coefficient is calculated considering the effects of geometry and friction losses:

$$C_{d\,final} = \frac{C_{deq\,prim}}{\sqrt{1+\xi_{inj} C_{deq\,prim}^2 \frac{K_{prim}^2}{C^2}}} \tag{4}$$

where $C = R_{prim} / r_s$. The friction coefficient, $\lambda = 0{,}3164\,Re^{-0.25}$, through the tangential channels depends on the flow Reynolds number:

$$Re = \frac{2\dot{m}_i}{\pi n_f r_f \rho \upsilon} \tag{5}$$

and the total friction loss in the injector is determined by:

$$\xi = \xi_o + \lambda \frac{l_f}{2r_f} \tag{6}$$

where the initial loss coefficient ξ_o , is determined from Figure 3.

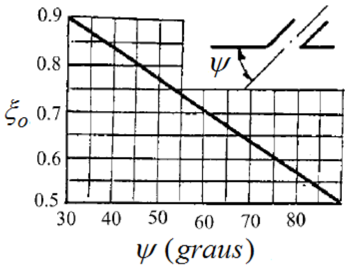

Figure 3. Initial viscous loss coefficient versus inclination of tangencial channels.

The inclination of the tangential channel, ψ , is obtained from relationship:

$$\psi = 90° - \tan^{-1}\frac{r_{cv}}{l_f} \tag{7}$$

For a given tangential inclination of the channel, there is a particular ξ_o , then the semi-cone angle of the primary chamber (Vasquez, 2011) is:

$$sin\alpha = \frac{2C_{d\ final} K_{prim} Z}{\left(1+\sqrt{1-\varepsilon_{prim}}\right)\sqrt{1-\xi_{inj} C_{d\ final}^2 \frac{K_{prim}^2}{C^2}}} \tag{8}$$

The spray cone semi-angle in the secondary chamber is derived in a similar fashion to the primary chamber (8), but using the following relation for the geometry of the secondary chamber:

$$K_{\sec} = \frac{A_{s\sec} R_{\sec}}{A_f r_{s\sec}} = \frac{\left(r_{s\sec}^2 - r_{sprimext}^2\right)\left(r_{cv\sec} - r_{f\sec}\right)}{n_{f\sec} r_{f\sec}^2 \left(r_{s\sec} - r_{sprimext}\right)} \tag{9}$$

The value of ε for the secondary chamber is obtained also using Figure 2. In Vasquez 2011, the following relationship was obtained for the final discharge coefficient,

$$C_{d\sec(\varepsilon_{\sec})} = \varepsilon_{\sec}\sqrt{\frac{\varepsilon_{\sec}\left(r_{s\sec}^2 - r_{sprimext}^2\right)}{r_{s\sec}^2\left(2-\varepsilon_{\sec}\right) + r_{sprimext}^2\left(\varepsilon_{\sec}\right)}} \tag{10}$$

To determine the semi-cone angle formed at the outlet of the secondary chamber equation (8) is used.

In the case of a dual centrifugal injector, the collision of the two spray cones formed generates another spray cone whose angle can be obtained using the momentum conservation equation. Assuming steady non viscous flow conditions, uniform pressure, uniform exit velocity at the orifices and no body forces give the equilibrium equations in the radial and axial components are:

$$\dot{m}_{prim} u_{prim} + \dot{m}_{\sec} u_{\sec} = \left(\dot{m}_{prim} + \dot{m}_{\sec}\right) u_{final} \tag{11a}$$

$$\dot{m}_{prim}\, v_{prim} + \dot{m}_{\sec}\, v_{\sec} = \left(\dot{m}_{prim} + \dot{m}_{\sec}\right) v_{final} \quad (11b)$$

The resulting angle is defined as;

$$\gamma = \tan^{-1}\left(\frac{v_{final}}{u_{final}}\right) = \tan^{-1}\left(\frac{\dot{m}_{prim}\, v_{prim} + \dot{m}_{\sec}\, v_{\sec}}{\dot{m}_{prim}\, u_{prim} + \dot{m}_{\sec}\, u_{\sec}}\right) \quad (12)$$

Finally, this equation can be written as a function of semi-cone angles of the inner chamber (α) and external (β).

$$\gamma = \tan^{-1}\left(\frac{\dot{m}_{prim} V_{prim}\, sen\,\alpha + \dot{m}_{\sec} V_{\sec}\, sen\,\beta}{\dot{m}_{prim} V_{prim} \cos\alpha + \dot{m}_{\sec} V_{\sec} \cos\beta}\right) \quad (13)$$

The equation (13), is valid in the case of external collision of the jets generated by the primary and secondary chamber.

2.2 Semi-empirical models

Tanasawa and Kobayasi (Lefebvre, 1989) considered only geometrical parameters and obtained a semi-empirical equation to calculate the spray semi-angle:

$$2\alpha = 180° - 2\arctan\left[\frac{4}{\pi} K\left(1.37 + 26.9 e^{-11.1\left(\sqrt{A_i}/d_s\right)}\right)\right] \quad (14)$$

Rizk-Lefebvre, these researchers studied the behavior of effects on the properties of the liquid, the geometrical parameters of the injector, and the injection pressure on the thickness of the liquid film, with these observations they derived the following equation dimensionally correct for the spray angle:

$$2\alpha = 6K^{-0.15}\left(\frac{\Delta P d_s^2 \rho}{\upsilon^2}\right)^{0.11} \quad (15)$$

Benjamin (1998) validated its equation using a database and modified the coefficients indicated by Rizk and Lefebvre for large size injectors and obtained the following expression:

$$2\alpha = 9.75K^{-0.287}\left(\frac{\Delta P d_s^2 \rho}{\upsilon^2}\right)^{0.067} \quad (16)$$

3. EXPERIMENTAL METHODOLOGY

3.1 The injector

Figure 4 shows a scheme and Figure 5 shows a computer cut view and a photo of the dual centrifugal injector.

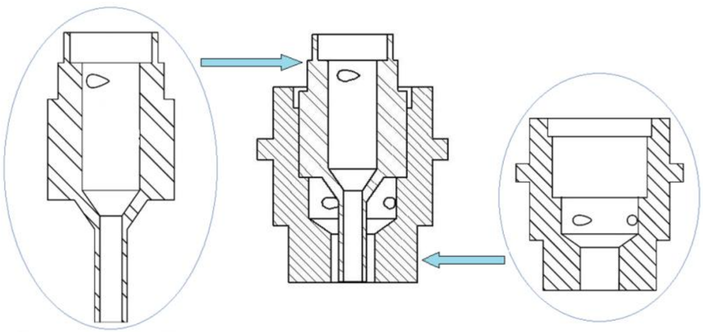

Primary chamber   secondary chamber

Figure 4. Scheme of the dual centrifugal injector.

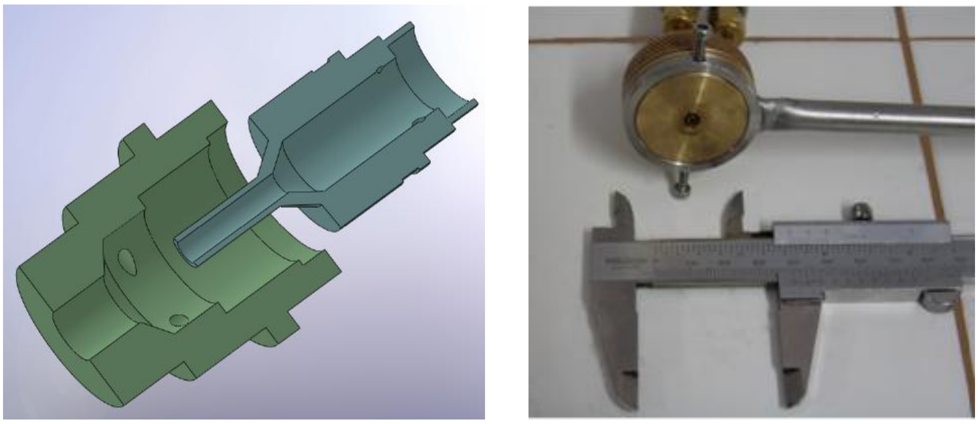

Figura 5. Cut view and photo of the injector.

Table 1. shows a summary of the operation and geometric parameters used in the design of the dual centrifugal injector.

Table 1. Parameters of the dual centrifugal injector.

Parameter	**Primary chamber**		**Secondary chamber**	
Operating pressure [Pa]	ΔP	2×10^{5}	ΔP	2×10^{5}
Mass flow rate [kg/s]	$\dot{m}_{prim}$	10.3×10^{-3}	$\dot{m}_{\sec}$	16×10^{-3}
Discharge coefficient	$C_{d\,prim}$	0.1961	$C_{d\,\sec}$	0.0922
Inner diameter of the outlet nozzle [m]	$d_{s\,prim}$	1.83×10^{-3}	$d_{s\,\sec}$	4.28×10^{-3}
Number of tangential channels	$n_{f\,prim}$	2	$n_{f\,\sec}$	4
Tangencial channel diameter [m]	$d_{f\,prim}$	1×10^{-3}	$d_{f\,\sec}$	1×10^{-3}
Outer diameter of the nozzle outlet [m]	$d_{sprimext}$	2.70×10^{-3}	$d_{s\sec ext}$	12.50×10^{-3}
Injector geometric constants	K_{prim}	3.45	K_{sec}	5

3.2 Physical-chemical parameters of the biofuels used

Physical-chemical properties of biofuels were measured experimentally using the method of pycnometry to determine density, the ring method to determine the surface tension and a viscometer of Otswald Cannon Fenske was used to determine the viscosity of these biofuels. Table 2 shows a summary of the physical-chemical parameters determined for the two biofuels used in this research.

Table 2. Physical-chemical properties of the biofuels.

Biofuel	**Density [kg/m³]**	**Viscosity [N s/m²]**	**Surface tension [N/m]**
Etanol 96%	806.7	1.24E-03	0.024
Soy Biodiesel B100	875.7	4.88E-03	0.028

3.3 Spray angle measurement

Figure 6.a shows the experimental setup used for measuring the spray cone angle by photographic techniques. The pictures were obtained by a Sony DSC-F828 digital camera, with 8 megapixels of effective resolution, or 3264×2448 pixels. The images can be captured in RAW, JPEG or TIFF formats.

The image presented in Figure 4.a shows, in the left side, the support with marks to indicate a known length to be used as a reference to relate the number of pixels and the true length of the image, allowing to determine the experimental values of the spray cone angles from the respective images.

Figure 6.b shows the GUI (Graphical User Interface) developed in Matlab language, especially written for this work to process spray images. The use of this GUI is relatively simple and the images can be treated in JPEG, TIFF or BMP formats.

After taking and selecting the appropriate images, the image processing is done with the GUI developed for this purpose, as shown in Figure 7. Finally, the experimental values of the cone angles of these images are registered. After data collection and treatment the experimental curves are obtained and compared to the theoretical data.

a)

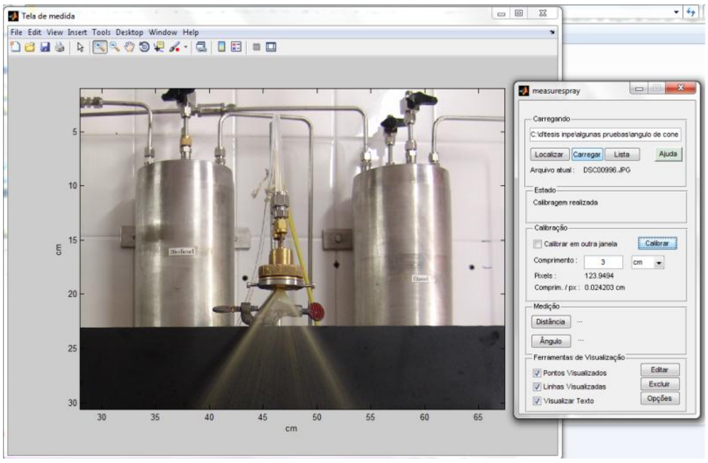

b)

Figure 6. a) Experimental setup and b) GUI for image processing.

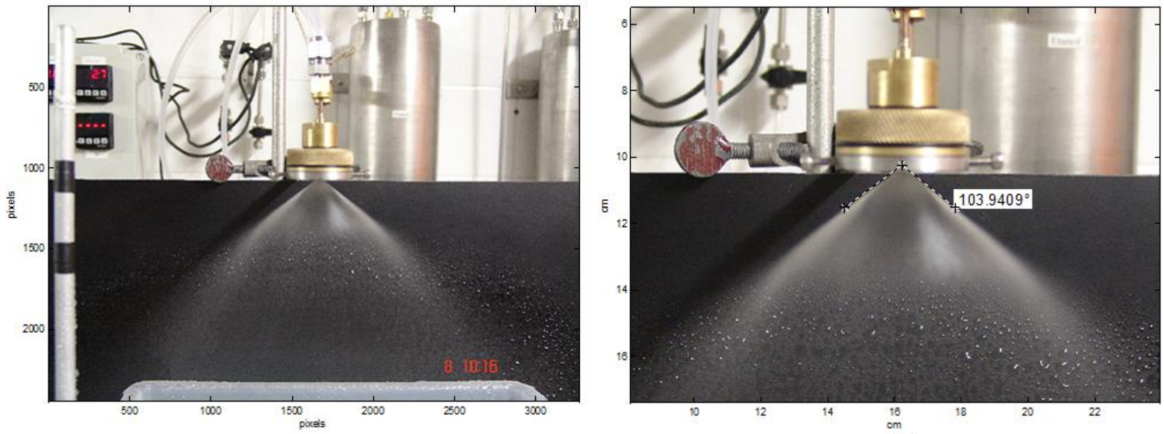

a) **b)**

Figure 7. Pictures of the cone angle measurement with image processing software developed: a) not calibrated image, b) calibrated image showing experimental value.

4. EFFECTS OF INJECTION PRESSURE ON SPRAY CONE ANGLES

4. 1 Primary chamber

Figures 8.a and 8.b compare the theoretical, semi-empirical and experimental values, as described by Vasquez (2011), of the spray cone angles for injection of hydrated ethanol and soy biodiesel, respectively, in the primary chamber of the injector as a function of the injection pressure (gauge pressure).

a)

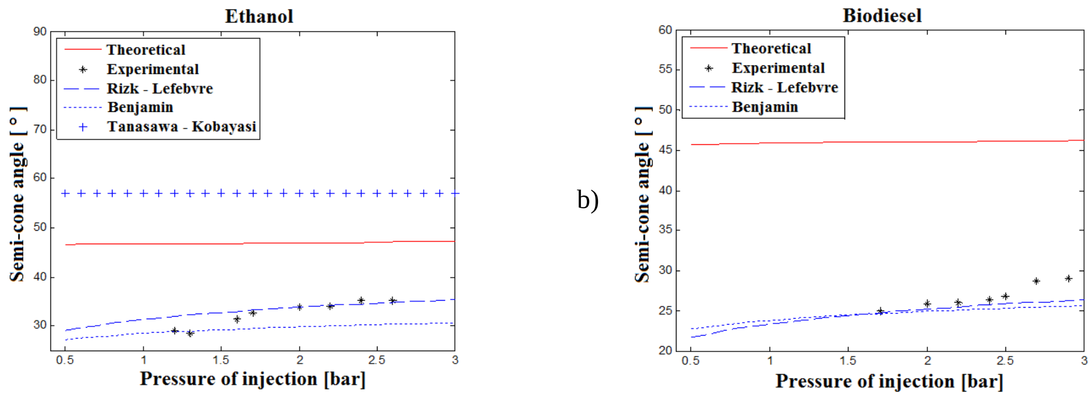

Figure 8. Cone angle generated in the primary chamber of the injector to a) hydrated ethanol; b) soy biodiesel.

4.2 Secondary chamber

Figures 9.a and 9.b compare the theoretical, semi-empirical and experimental values of the spray cone angle for injection of hydrated ethanol and soy biodiesel, respectively, in the secondary chamber of the injector, as a function of injection pressure (gauge pressure). It can be observed a slight increase of the cone angle with the injection pressure for the two liquid and that the cone angle of the ethanol is greater than the biodiesel, i.e., varies inversely with the viscosity of the liquid.

Note that for both primary and secondary chambers the behavior of cone angle with operating pressure is influenced by the physical-chemical properties of the injected liquid and the geometrical parameters of both chambers of the dual centrifugal injector.

a)

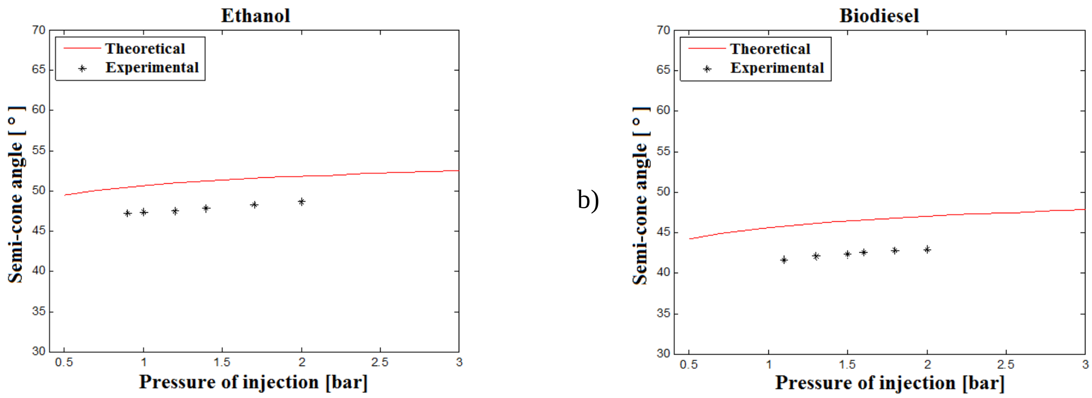

Figura 9. Behavior of the cone angle generated in the secundary chamber of the injector to a) hydrated ethanol; b) soy biodiesel.

4.3 External mixture of ethanol and biodiesel

Figure 10.a shows the spray cone angle formed by injection of ethanol in the primary chamber and soy biodiesel B100 in the secondary chamber.

It can be verified in Figure 10.b that the theoretical cone angle is about 30% larger than the experimental cone angle in the case of the mixture. This difference is due to neglecting viscous effects at the theoretical equation for the case of the secondary chamber.

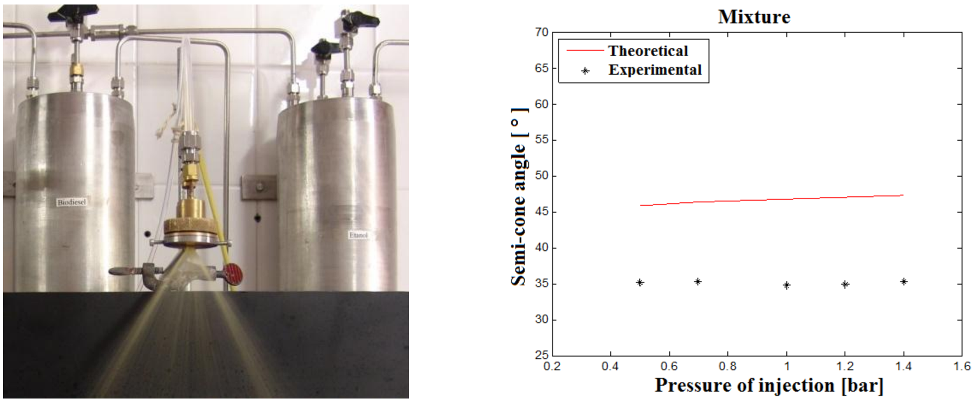

a) b)

Figura 10 - Comparison of experimental and theoretical values of the spray cone angle using a mixture of ethanol and biodiesel.

5. CONCLUSIONS

The Rizt-Lefebvre semi-empirical formulation gave the best estimates of spray cone angles generated by the biofuels injected in the primary chamber, indicating that liquid properties and geometrical parameters of the injector have an important role to determine the spray cone angle.

In the case of injection of ethanol in the primary chamber and injection of biodiesel in the secondary chamber, the theoretical cone angle was about 30% larger than the experimental cone angle. This difference is due to neglecting the viscous effects in the theoretical equation used, especially in the secondary chamber.

The cone angles formed by injection of biofuels in both chambers increase with injection pressure. The spray cone angles formed by ethanol injection is greater than the spray cone angle formed by biodiesel injection, consequence of the larger viscosity of biodiesel.

6. ACKNOWLEDGEMENTS

The authors acknowledge FAPESP for financial support.

7. REFERENCES

Ballester, J. and Dopazo, C., 1994. “Discharge coefficient and spray angle measurements for small pressure-swirl nozzles”. *Atomization and Sprays*, Vol. 4, pp. 351 – 367.

Chen, S. K., lefebvre, A. H. and Rollbuhler, J., 1992. “Factors influencing the effective spray cone angle of pressure-swirl atomizers”. *Journal of Engineering for Gas Turbines and Power*, Vol. 114, pp. 97-103.

Ding-yuan, L., 1987. Study and the characteristic of the spray angle in pressure swirl spray atomisation, *Applied Mathematics and Mechanics*, Vol. 8, n. 5.

Inamura, T.; Tamura, H.; Sakamoto, K., 2003. Characteristics of liquid film and spray injected from swirl coaxial injector, *Journal of Propulsion and Power*, vol. 19, n. 4, pp. 632-639.

Lefebvre, A. H., 1989. *Atomization and Sprays*, Hemisphere, New York.

Ommi, F., Nekofar, K., Kargar, A. and Movahed, E., 2009. “Experimental investigation of characteristics of a double-base swirl injector in a liquid rocket propellant Engine”. *Leonardo Journal of Sciences*, Vol. 14, pp. 92 – 111.

Ortmann, J. and Lefebvre, A. H., 1985. “Fuel distributions from pressure-swirl atomizers”. *Journal Propulsion and Power*, Vol. 1, n. 1, pp. 11-15.

Vásquez, A. R., 2011, *Desenvolvimento de um injetor centrífugo dual para biocombustíveis líquidos*. Dissertação (Mestrado em propulsão e combustão), Instituto Nacional de Pesquisas Espaciais, São José dos Campos, SP, Brazil.

8. RESPONSIBILITY NOTICE

The authors are the only responsible for the printed material included in this paper.